Yields and polarizations of prompt J/ψ and $\psi(2S)$ production in hadronic collisions

Hua-Sheng Shao^{a*}**,Hao Han**^{a}**,Yan-Qing Ma**^{b,c}**,Ce Meng**^{a}**, Yu-Jie Zhang**^{d}**, Kuang-Ta Chao**^{a,c,e}

^{a}*School of Physics and State Key Laboratory of Nuclear Physics and Technology, Peking University, Beijing 100871, China*
^{b}*Maryland Center for Fundamental Physics, University of Maryland, College Park, Maryland 20742, USA*
^{c}*Center for High Energy Physics, Peking University, Beijing 100871, China*
^{d}*Key Laboratory of Micro-nano Measurement-Manipulation and Physics (Ministry of Education) and School of Physics, Beihang University, Beijing 100191, China*
^{e}*Collaborative Innovation Center of Quantum Matter, Beijing 100871, China*
E-mail: huasheng.shao@cern.ch,hao.han@pku.edu.cn,yqma@umd.edu, mengce75@pku.edu.cn,nophy0@gmail.com,ktchao@pku.edu.cn

ABSTRACT: We give predictions of J/ψ and $\psi(2S)$ yields and polarizations in prompt production at hadron colliders based on non-relativistic QCD factorization formula. We calculate short-distance coefficients of all important color-octet intermediate channels as well as color-singlet channels up to $\mathcal{O}(\alpha_S^4)$, i.e. next-to-leading order in α_S. For prompt J/ψ production, we also take into account feeddown contributions from χ_{cJ}(J=0,1,2) and $\psi(2S)$ decays. Color-singlet long-distance matrix elements (LDMEs) are estimated by using potential model, and color-octet LDMEs are extracted by fitting the Tevatron yield data only. The predictions are satisfactory for both yields and polarizations of prompt J/ψ and prompt $\psi(2S)$ production at the Tevatron and the LHC. In particular, we find our predictions for polarizations of prompt J/ψ production have only a little difference from our previous predictions for polarizations of direct J/ψ production.

KEYWORDS: NLO Computations, Hadronic Colliders.

---

*Present address: *PH Department, TH Unit, CERN, CH-1211, Geneva 23, Switzerland.*

Contents

1. Introduction

Heavy quarkonium physics provides an ideal laboratory to study QCD at the interplay between perturbative and non-perturbative domains. Because of the large samples of J/ψ and $\psi(2S)$ accumulated at the LHC, it is an opportune moment to study the quarkonium production mechanism. To this end, understanding the polarization of produced quarkonium is an attractive and important issue [1, 2].

At the Tevatron, the polarization observable λ_θ (or α) for both of prompt J/ψ and prompt $\psi(2S)$ in their helicity frame measured by CDF Collaboration [3] are close to 0, which are in contradiction with the prediction of transverse polarization at the leading order (LO) in non-relativistic QCD (NRQCD) [4]. In the past a few years, three groups [5, 6, 7] reported their independent analyzes of J/ψ polarizations at the next-to-leading order (NLO) level in α_S. Although the short-distance coefficients (SDCs) are consistent with each other, the three groups give three different versions for the polarization prediction because different treatments are used in the extractions of non-perturbative color-octet (CO) long-distance matrix elements (LDMEs). Specifically, both ref. [5] and ref. [7] claim that the NLO NRQCD will necessarily give a transversely polarized prediction for prompt J/ψ production; while the work

by some of the present authors [6] give a possible explanation for the J/ψ polarization issue by finding that the transversely polarized contributions from ${}^3S_1^{[8]}$ and ${}^3P_J^{[8]}$ channels cancel each other. A similar cancelation between ${}^3S_1^{[8]}$ and ${}^3P_J^{[8]}$ channels for yield was also found earlier in ref. [8]. The consequence of these cancelations is that the ${}^1S_0^{[8]}$ channel will dominate, which results in an unpolarized prediction. Note that, the crucial point to get these cancelations is the introduction of a relatively large p_T cutoff for data in the lower p_T region.

In the high p_T region, however, large logarithms like $\ln(p_T^2/m_c^2)$ may ruin the convergence of perturbative expansion, thus resummation of these large logarithmic terms are needed. This can be done by using DGLAP evolution equations to resum terms in the leading power in $1/p_T$ expansion, and using double parton evolution equations derived in ref. [9] to resum terms in the next-to-leading power in $1/p_T$ expansion. The first goal is achieved recently [10]. By combining the NLO NRQCD result with the leading power resummation, authors in ref. [10] find that contributions from ${}^3S_1^{[8]}$ and ${}^3P_J^{[8]}$ channels should be almost canceled with each other and the produced J/ψ is almost unpolarized, which is similar to our conclusion in ref. [6]. This is encouraging because it implies that the qualitative results in the NLO NRQCD calculation are not changed by resummation.

Based on the NLO NRQCD calculation, a data-driven method is employed in ref. [11] to fit CO LDMEs. By investigating the behaviour of $\chi^2/d.o.f.$ for different p_T cutoff, the authors push the p_T cutoff for $\psi(2S)$ to even larger values, say, about 12 GeV. Then they found that the $\psi(2S)$ production is dominated by the ${}^1S_0^{[8]}$ channel and the polarization data of $\psi(2S)$ production can be explained, which is similar to the explanation of J/ψ polarization in refs. [6, 10]. Therefore, it seems possible that the polarizations of J/ψ and $\psi(2S)$ can be explained in a unified way.

However, in ref. [6], as well as in refs. [5, 10], only the direct J/ψ production contribution is considered. An estimation of the impact of feeddown contributions to J/ψ polarization is given in ref. [12], where it was pointed out that the feeddown contributions should not change the polarization result too much. Yet, to be precise, it should be better to include the feeddown contributions rigorously since they may contribute a substantial amount of prompt J/ψ production. Hence, the purpose of the present article is to do a comprehensive analysis for prompt J/ψ production by including the feeddown contributions from χ_{cJ} and $\psi(2S)$ decays. Meantime, we also give predictions of yields and polarizations for prompt $\psi(2S)$.

The remaining context is organized as follows. We first fix our strategy for estimating the LDMEs in section 2, and then give our predictions for the yields and polarizations of $\psi(2S)$ and J/ψ in the next two sections. A summary will be given in the last section.

J/ψ	$\psi(2S)$	χ_{c0}	χ_{c1}	χ_{c2}
3.097	3.686	3.415	3.511	3.556

Table 1: Physical masses (in unit of GeV) of various charmonia [18].

2. Strategy for estimating LDMEs

2.1 General setup

Before going ahead, we first list some details that are used in this article. The helicity-summed yields are calculated following the way mentioned in refs. [8, 13, 14], while the method of the polarisation is described in refs. [6, 15, 16].

Cross section for a quarkonium $\mathcal{Q}$ production in pp collision can be expressed as [4]

$$\sigma(pp \to \mathcal{Q} + X) = \sum_n \hat{\sigma}(pp \to Q\bar{Q}[n] + X) \times \langle \mathcal{O}^{\mathcal{Q}}(n) \rangle, \qquad (2.1)$$

where $\hat{\sigma}(pp \to Q\bar{Q}[n] + X)$ are SDCs for producing a heavy quark pair $Q\bar{Q}$ with the quantum number n, and $\langle \mathcal{O}^{\mathcal{Q}}(n) \rangle$ is a LDME for $\mathcal{Q}$. SDCs can be computed in perturbative QCD as

$$\hat{\sigma}(pp \to Q\bar{Q}[n] + X) = \sum_{a,b} \int dx_1 dx_2 d\text{LIPS} f_{a/p}(x_1) f_{b/p}(x_2)$$
$$\times |M(ab \to Q\bar{Q}[n] + X)|^2, \qquad (2.2)$$

where the symbols a and b represent all possible partons, x_1 and x_2 are light-cone momentum fractions, $d\text{LIPS}$ is the lorentz-invariant phase space measure, and $f_{a/p}(x_1)$ and $f_{b/p}(x_2)$ are parton distribution functions (PDFs) for partons a and b in the initial colliding protons.

In this article, we have included all important $c\bar{c}$ Fock states, ${}^3S_1^{[1]}$, ${}^1S_0^{[8]}$, ${}^3S_1^{[8]}$ and ${}^3P_J^{[8]}$ for J/ψ and $\psi(2S)$, ${}^3S_1^{[8]}$ and ${}^3P_J^{[1]}$ for χ_{cJ}. All corresponding SDCs are calculated up to $\mathcal{O}(\alpha_S^4)$, i.e. NLO in α_S. We use CTEQ6M [17] as our default PDF. The mass of charm quark is fixed to be $m_c = 1.5\text{GeV}$, and an analysis of uncertainties from choosing charm quark mass can be found in ref. [8]. The renormalization and factorization scales are $\mu_R = \mu_F = \sqrt{(2m_c)^2 + p_T^2}$, while the NRQCD scale is $\mu_\Lambda = m_c$. Since cross sections of charmonia are decreasing with high powers of their p_T, we should consider the p_T spectrum shiftting in the decay of $\mathcal{Q}_1 \to \mathcal{Q}_0 + X$ approximately by $p_T^{\mathcal{Q}_0} = \frac{M_{\mathcal{Q}_0}}{M_{\mathcal{Q}_1}} p_T^{\mathcal{Q}_1}$ [8], where $M_{\mathcal{Q}_0}$ and $M_{\mathcal{Q}_1}$ are physical masses for quarkonia $\mathcal{Q}_0$ and $\mathcal{Q}_1$ respectively. Masses of relevant charmonia in our article are shown in Table 1. Table 2 gives the branching ratios for various decay processes involved in this article.

decay channel	branching ratio ($\times 10^{-2}$)
$J/\psi \to \mu^+\mu^-$	5.93
$\psi(2S) \to \mu^+\mu^-$	0.75
$\psi(2S) \to J/\psi + X$	57.4
$\psi(2S) \to J/\psi\pi^+\pi^-$	34.0
$\psi(2S) \to \chi_{c0} + \gamma$	9.84
$\psi(2S) \to \chi_{c1} + \gamma$	9.3
$\psi(2S) \to \chi_{c2} + \gamma$	8.76
$\chi_{c0} \to J/\psi + \gamma$	1.28
$\chi_{c1} \to J/\psi + \gamma$	36.0
$\chi_{c2} \to J/\psi + \gamma$	20.0

Table 2: Branching ratios of various decay processes involved in this article [18].

$p_{T\text{cut}}^{\psi(2S)}$(GeV)	$M_{0,r_0}^{\psi(2S)}(\times 10^{-2}\text{GeV}^3)$	$M_{1,r_1}^{\psi(2S)}(\times 10^{-2}\text{GeV}^3)$	$\chi^2/d.o.f$
5	1.3754 ± 0.118931	0.159987 ± 0.0117348	$37.2068/16 = 2.32542$
6	1.93677 ± 0.17044	0.128511 ± 0.0135506	$14.0112/14 = 1.0008$
7	2.23162 ± 0.23115	0.109918 ± 0.0155178	$7.21501/12 = 0.601251$
8	2.253154 ± 0.301835	0.100531 ± 0.0175978	$5.46679/10 = 0.546679$
9	2.7258 ± 0.401123	0.0932409 ± 0.0201979	$4.92587/8 = 0.615734$
10	3.23067 ± 0.58727	0.0763209 ± 0.0247166	$3.37617/6 = 0.562696$
11	3.81594 ± 0.784395	0.0585894 ± 0.0293102	$2.10933/5 = 0.421866$
12	3.67631 ± 1.00394	0.0625013 ± 0.0341653	$2.05968/4 = 0.514919$
13	3.48695 ± 1.30212	0.0673741 ± 0.0402811	$2.00752/3 = 0.669175$
14	3.02071 ± 1.7219	0.0784274 ± 0.0483324	$1.83628/2 = 0.918141$
15	1.04558 ± 2.34914	0.121791 ± 0.0597233	$0.308538/1 = 0.308538$

Table 3: The values of $M_{0,r_0}^{\psi(2S)}$ and $M_{1,r_1}^{\psi(2S)}$ by fitting the CDF data [26] with different $p_{T\text{cut}}$, where $r_0 = 3.9, r_1 = -0.56$.

The polarisation observable λ_θ for $J/\psi(\psi(2S))$ is defined as [19, 20]

$$\lambda_\theta = \frac{d\sigma_{11} - d\sigma_{00}}{d\sigma_{11} + d\sigma_{00}}, \tag{2.3}$$

where $d\sigma_{ij}(i, j = 0, \pm 1)$ is the ij component in the spin density matrix formula for $J/\psi(\psi(2S))$. The full spin correlation of χ_{cJ}'s spin density matrix element and J/ψ's spin density matrix element including E1, M2 and E3 transitions has been explored in eq. (C4) of ref. [12]. We use the normalized M2 amplitude $a_2^{J=1} = -6.26 \times 10^{-2}$ for $\chi_{c1} \to J/\psi + \gamma$, and the normalized M2 and E3 amplitudes $a_2^{J=2} = -9.3 \times 10^{-2}$ and $a_3^{J=2} = 0$ for $\chi_{c2} \to J/\psi + \gamma$, which are measured by CLEO collaboration [21].

From the eq. (C4) of ref. [12], we notice that the λ_θ is squared-amplitude dependent. Hence, these extra spin-flip effects due to M2 and E3 transitions are negligible. We still keep it here since no extra effort is needed.

2.2 LDMEs estimation

Because of spin symmetry, LDMEs $\langle \mathcal{O}^{\chi_{cJ}}(^3S_1^{[8]}) \rangle$ and $\langle \mathcal{O}^{\chi_{cJ}}(^3P_J^{[1]}) \rangle$ for χ_{cJ} have the relation

$$\langle \mathcal{O}^{\chi_{cJ}}(^3S_1^{[8]}) \rangle = (2J+1)\langle \mathcal{O}^{\chi_{c0}}(^3S_1^{[8]}) \rangle, \tag{2.4}$$

$$\langle \mathcal{O}^{\chi_{cJ}}(^3P_J^{[1]}) \rangle = (2J+1)\langle \mathcal{O}^{\chi_{c0}}(^3P_0^{[1]}) \rangle. \tag{2.5}$$

Color-singlet LDME $\langle \mathcal{O}^{\chi_{c0}}(^3P_0^{[1]}) \rangle$ can be estimated by the derivation of wavefunction at origin $R'(0)$ via

$$\langle \mathcal{O}^{\chi_{c0}}(^3P_0^{[1]}) \rangle = 2N_c \frac{3}{4\pi}|R'(0)|^2, \tag{2.6}$$

where $|R'(0)|^2 = 0.075 \text{ GeV}^5$ is calculated in ref. [22] by using potential model. The remaining CO LDME $\langle \mathcal{O}^{\chi_{c0}}(^3S_1^{[8]}) \rangle$ should be determined by fitting experimental data. In ref. [14], we used p_T spectrum of $\sigma_{\chi_{c2} \to J/\psi\gamma}/\sigma_{\chi_{c1} \to J/\psi\gamma}$ measured by CDF [23] in our fitting procedure, and we got

$$\langle \mathcal{O}^{\chi_{c0}}(^3S_1^{[8]}) \rangle = (2.2^{+0.48}_{-0.32}) \times 10^{-3} \text{GeV}^3, \tag{2.7}$$

which is consistent with later studies [7, 16, 24]. Moreover, we want to emphasize that this value is insensitive to p_T cutoff in our fit, especially when $p_T > 7\text{GeV}$.

Similarly, CS LDMEs for J/ψ and $\psi(2S)$ can also be estimated by potential model [22],

$$\langle \mathcal{O}^{J/\psi}(^3S_1^{[1]}) \rangle = 2N_c \frac{3}{4\pi}|R_{J/\psi}(0)|^2 = 1.16 \text{ GeV}^3, \tag{2.8}$$

$$\langle \mathcal{O}^{\psi(2S)}(^3S_1^{[1]}) \rangle = 2N_c \frac{3}{4\pi}|R_{\psi(2S)}(0)|^2 = 0.76 \text{ GeV}^3, \tag{2.9}$$

although their precise values are in fact irrelevant in our analysis because their corresponding SDCs are too small in our interested p_T regime. The determination of three unknown CO LDMEs for $J/\psi(\psi(2S))$ is more complicated and involved. Based on our previous studies [6, 8, 13], we summarize the following facts:

- In the regime $p_T > 4m_c$, the short-distance coefficient of P-wave CO Fock state $^3P_J^{[8]}$ can be nicely decomposed into a linear combination of the short-distance coefficients of $^1S_0^{[8]}$ and $^3S_1^{[8]}$,

$$d\hat{\sigma}(^3P_J^{[8]}) = r_0 \frac{d\hat{\sigma}(^1S_0^{[8]})}{m_c^2} + r_1 \frac{d\hat{\sigma}(^3S_1^{[8]})}{m_c^2}. \tag{2.10}$$

r_0 and r_1 changes slightly with rapidity interval but almost not changes with the center-of-mass energy $\sqrt{S}$ (see table I in ref. [13]). This makes it difficult to extract three independent CO LDMEs by fitting helicity-summed yields data at hadron colliders. Instead, one is restricted to be able to extract two linear combinations of three CO LDMEs within convincing precision. They are denoted as

$$M_{0,r_0}^{J/\psi(\psi(2S))} \equiv \langle \mathcal{O}^{J/\psi(\psi(2S))}(^1S_0^{[8]}) \rangle + r_0 \frac{\langle \mathcal{O}^{J/\psi(\psi(2S))}(^3P_0^{[8]}) \rangle}{m_c^2}, \qquad (2.11)$$

$$M_{1,r_1}^{J/\psi(\psi(2S))} \equiv \langle \mathcal{O}^{J/\psi(\psi(2S))}(^3S_1^{[8]}) \rangle + r_1 \frac{\langle \mathcal{O}^{J/\psi(\psi(2S))}(^3P_0^{[8]}) \rangle}{m_c^2}. \qquad (2.12)$$

Because $d\hat{\sigma}(^1S_0^{[8]})$ and $d\hat{\sigma}(^3S_1^{[8]})$ have mainly p_T^{-6} and p_T^{-4} behaviour respectively, values of $M_{0,r_0}^{J/\psi(\psi(2S))}$ and $M_{1,r_1}^{J/\psi(\psi(2S))}$ can roughly indicate the relative importance of p_T^{-6} and p_T^{-4} components. Using the Tevatron yields data [25, 26] with $p_T > 7\text{GeV}$, they are extracted as in ref. [8]

$$M_{0,r_0}^{J/\psi} = (7.4 \pm 1.9) \times 10^{-2}\text{GeV}^3, \qquad (2.13)$$

$$M_{1,r_1}^{J/\psi} = (0.05 \pm 0.02) \times 10^{-2}\text{GeV}^3, \qquad (2.14)$$

with $\chi^2/d.o.f = 0.33$ for J/ψ, and

$$M_{0,r_0}^{\psi(2S)} = (2.0 \pm 0.6) \times 10^{-2}\text{GeV}^3, \qquad (2.15)$$

$$M_{1,r_1}^{\psi(2S)} = (0.12 \pm 0.03) \times 10^{-2}\text{GeV}^3, \qquad (2.16)$$

with $\chi^2/d.o.f = 0.56$ for $\psi(2S)$, with $r_0 = 3.9$ and $r_1 = -0.56$. Inspired by the recent work [11], we are also trying to see what happens if we enlarge the p_T cutoff in our fit. With CDF data only [25, 26], we found values of $M_{0,r_0}^{\psi(2S)}$ and $M_{1,r_1}^{\psi(2S)}$ can be alternated by enlarging the p_T cutoff as shown in table 3, while it is not the case for J/ψ. When the cutoff is larger than 11GeV, we have relatively stable and minimal χ^2 value for $\psi(2S)$. We thus obtained another set of CO LDMEs for $\psi(2S)$ by choosing cutoff as $p_T = 11$ GeV,

$$M_{0,r_0}^{\psi(2S)} = (3.82 \pm 0.78) \times 10^{-2}\text{GeV}^3, \qquad (2.17)$$

$$M_{1,r_1}^{\psi(2S)} = (0.059 \pm 0.029) \times 10^{-2}\text{GeV}^3. \qquad (2.18)$$

For simplification, we will call this set of CO LDMEs as "set II" in the remaining context, while nothing will be labeled if we use the default one extracted from $p_T > 7\text{GeV}$ data in eqs. (2.15) and (2.16).

- The short-distance coefficient[1] $d\hat{\sigma}_{11}(^3P_J^{[8]})$ has the similar decomposition but into $d\hat{\sigma}_{11}(^1S_0^{[8]})$ and $d\hat{\sigma}_{11}(^3S_1^{[8]})$. The non-trivial thing is that coefficient of

---

[1]In this article, we only consider the helicity frame.

$d\hat{\sigma}_{11}(^3S_1^{[8]})$ in $d\hat{\sigma}_{11}(^3P_J^{[8]})$ decomposition is quite close to r_1 in $d\hat{\sigma}(^3P_J^{[8]})$ decomposition [6]. Hence, it still does not help a lot to fix the three independent CO LDMEs by including polarisation data [6]. Moreover, the value of $M_{1,r_1}^{J/\psi(\psi(2S))}$ almost control the weight of transverse component. The unpolarized data really require a (very) small $M_{1,r_1}^{J/\psi(\psi(2S))}$.

- We assume that all of the CO LDMEs are positive [6], which is in contrast with those given in refs. [5, 7] (see also refs. [27, 28, 29]).[2] Since r_1 in forward rapidity interval is smaller than that in central rapidity interval [13], a positive $\langle\mathcal{O}^{J/\psi(\psi(2S))}(^3P_0^{[8]})\rangle$ would imply that λ_θ in forward rapidity will be smaller than its value in the central rapidity. We will see later that this conclusion is confirmed by LHC data. Further more, in a recent study of $J/\psi + \gamma$ production [30], the authors found that positivity of CO LDMEs are needed to guarantee a physical cross section, while the sets of CO LDMEs in refs. [5, 7] result in unphysical negative cross section for $J/\psi + \gamma$ production at hadron colliders. It also supports our assumption.

Based on these reasons, we are trying to use only Tevatron yield data as input to give all yields and polarisation predictions for prompt J/ψ and $\psi(2S)$ production at hadron colliders. We use values of $M_{0,r_0}^{J/\psi(\psi(2S))}$ and $M_{1,r_1}^{J/\psi(\psi(2S))}$ in this section and vary $0 \leq \langle\mathcal{O}^{J/\psi(\psi(2S))}(^1S_0^{[8]})\rangle \leq M_{0,r_0}^{J/\psi(\psi(2S))}$ to estimate the three CO LDMEs. This variation and the errors in $M_{0,r_0}^{J/\psi(\psi(2S))}$, $M_{1,r_1}^{J/\psi(\psi(2S))}$ and $\langle\mathcal{O}^{\chi_{c0}}(^3S_1^{[8]})\rangle$ will be considered as theoretical uncertainties.

3. Prompt $\psi(2S)$ yields and polarizations

In this section, we discuss the prompt $\psi(2S)$ yields and polarisation at the Tevatron and the LHC. Experimentally, people can reconstruct $\psi(2S)$ via $\psi(2S) \to \mu^+\mu^-$ or $\psi(2S) \to J/\psi(\to \mu^+\mu^-)\pi^+\pi^-$. Unlike prompt J/ψ, there is no significant feeddown contribution to prompt $\psi(2S)$ production.
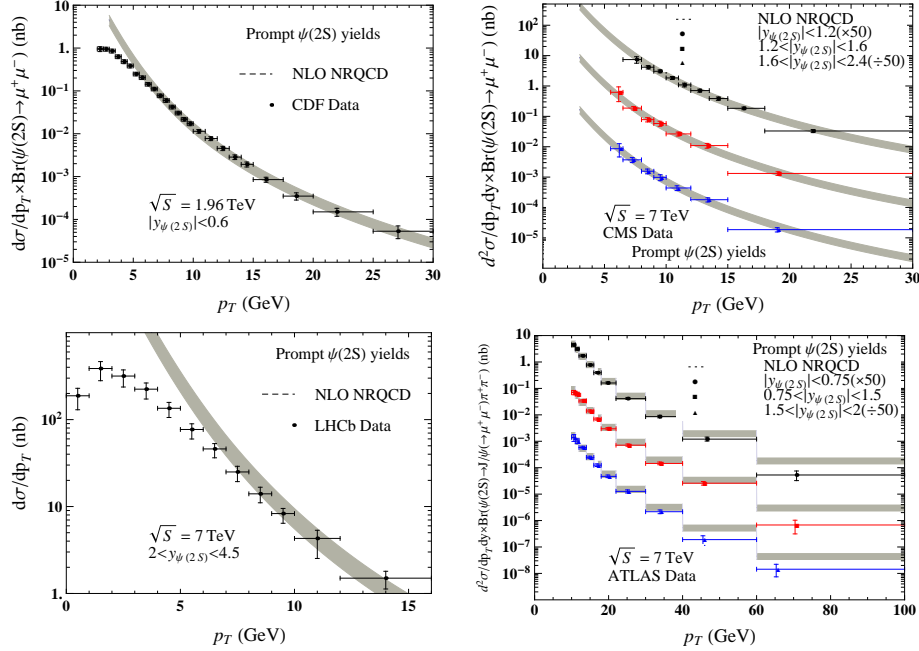
3.1 Yields

We update our numerical predictions for $\psi(2S)$ yields at the Tevatron and the LHC as several collaborations have released their prompt $\psi(2S)$ yields measurements [26, 31, 32, 33] in the past a few years. It is worthwhile to mention that one of the main uncertainty in experimental measurement comes from the unknown spin-alignment.

---

[2]Although the authors in ref. [7] used the same p_T cut and included the feed-down contribution in prompt J/ψ production, they tried to extract three independent CO LDMEs by including data in the forward-rapidity region. However, due to the correlation between the decompositions in the central and forward regions (see table I in ref. [13]), the uncertainties in the extracted three CO LDMEs might be underestimated and they got negative CO LDMEs.

Hence, it would be quite useful to give a theoretical prediction on polarisation, which will be presented in the next subsection. Our NLO NRQCD predictions for prompt $\psi(2S)$ yields are shown in figure 1 (using default set of CO LDMEs) and figure 2 (using set II of CO LDMEs). Our theoretical results are in good agreement with the experimental data at the LHC and Tevatron for the regime $p_T > p_{T\text{cut}}$, where we use $p_{T\text{cut}} = 7\text{GeV}$ in default set and $p_{T\text{cut}} = 11\text{GeV}$ in set II [Strictly speaking, ATLAS large p_T yields data favor our prediction on set II]. In the $p_T < p_{T\text{cut}}$ regime, experimental data tell us that there might be a significant non-perturbative smearing effect to violate the reliability of our fixed-order result. The error bands in our results represent our theoretical uncertainties, which are dominated by the uncertainties in CO LDMEs.

Figure 1: Comparison of NLO NRQCD (with the default set of CO LDMEs) and CDF [26],CMS [31], LHCb [32] and ATLAS [33] data for prompt $\psi(2S)$ yields.

3.2 polarizations

We are in the position to give the theoretical predictions of polarisation observable λ_θ for prompt $\psi(2S)$. We compare our NLO NRQCD results with the experimental data given by CDF [34] and CMS [35] collaborations in figure 3 (using default set of CO LDMEs) and figure 4 (using set II of CO LDMEs). As we discussed in section 2.2, a larger value of $M_{1,r_1}^{\psi(2S)}$ will result in a larger transverse component for prompt $\psi(2S)$. Hence, using our default set of CO LDMEs, the resulted λ_θ are much larger than the data (see figure 3), while values of λ_θ calculated by using set II of CO LDMEs
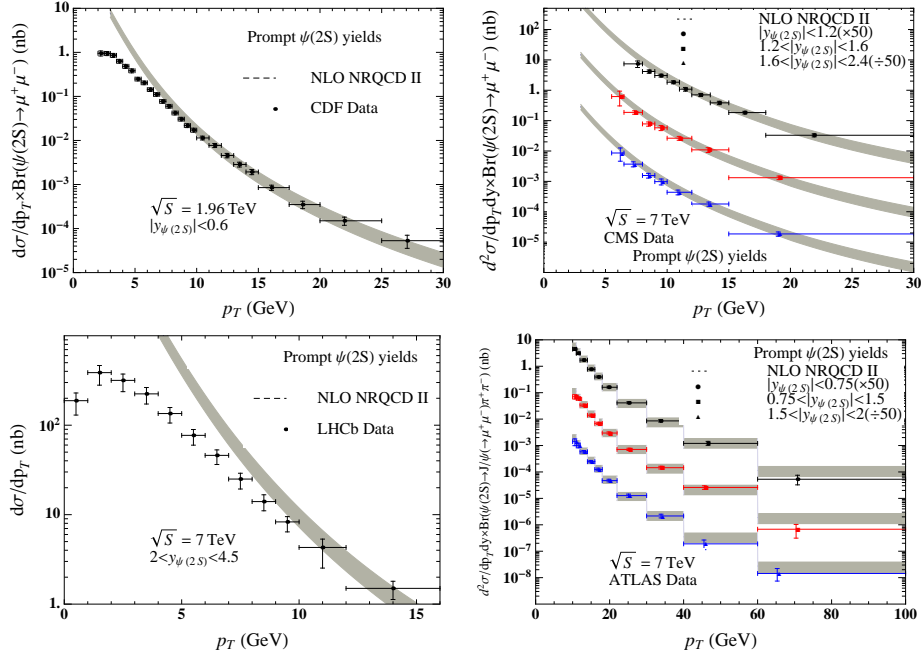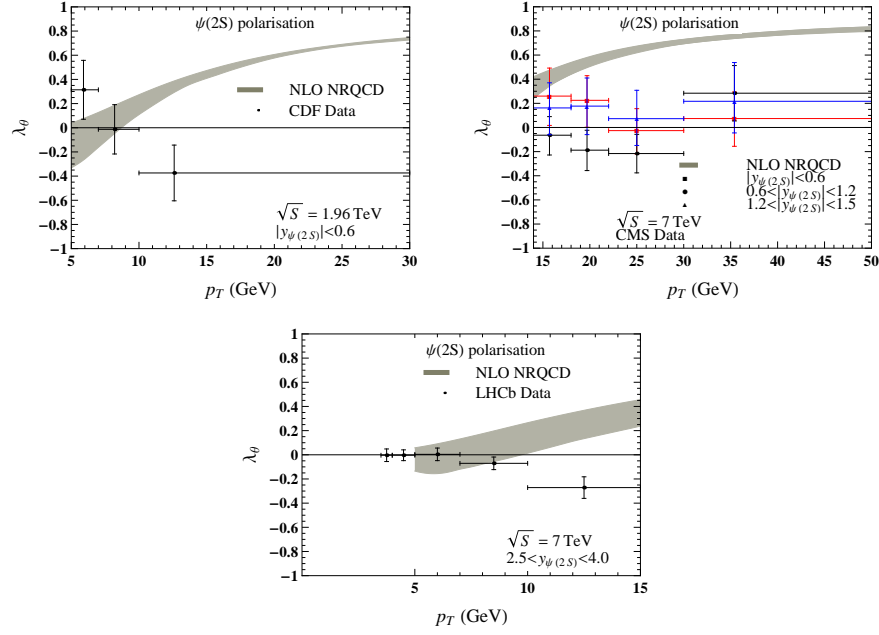
Figure 2: Comparison of NLO NRQCD (with the set II of CO LDMEs) and CDF [26], CMS [31], LHCb [32] and ATLAS [33] data for prompt $\psi(2S)$ yields.

in figure 4 can marginally describe the data. On the experimental side, there seems to be a little bit inconsistence between the CDF [34] data and the CMS [35] data, and the error bars are large. Therefore, a more precise measurement at the LHC is essential to clarify the difference in the future.

We would emphasize here that if we simply set $M_{1,r_1}^{\psi(2S)}$ to be zero and only keep $^1S_0^{[8]}$, it will of course result in unpolarized results for any polarisation observables in any frame, which is also noticed in refs. [8, 11].

4. Prompt J/ψ yields and polarizations

The prompt J/ψ production in hadronic collisions is more involved. It receives a significant contribution from χ_{cJ} and $\psi(2S)$ decay via $\chi_{cJ} \to J/\psi + \gamma$ and $\psi(2S) \to J/\psi + X$ respectively, which is usually called the feeddown contribution. J/ψ can be reconstructed quite well from its decay products, a muon pair. In our previous study [6], we did not include feeddown contribution in our J/ψ yields and polarisation predictions. We found there was still a parameter space for CO LDMEs to give an almost unpolarized theoretical prediction, though we were still unable to extract the three independent CO LDMEs unambiguously. More precisely, we need a cancellation happens between the transverse components of $^3S_1^{[8]}$ and $^3P_J^{[8]}$ to give an unpolarized result, which happens to be equivalent to need a (very) small $M_{1,r_1}^{J/\psi}$.

Figure 3: Comparison of NLO NRQCD (with the default set of CO LDMEs) and CDF [34], CMS [35] and LHCb [36] data for prompt $\psi(2S)$ polarisation λ_θ in helicity frame.
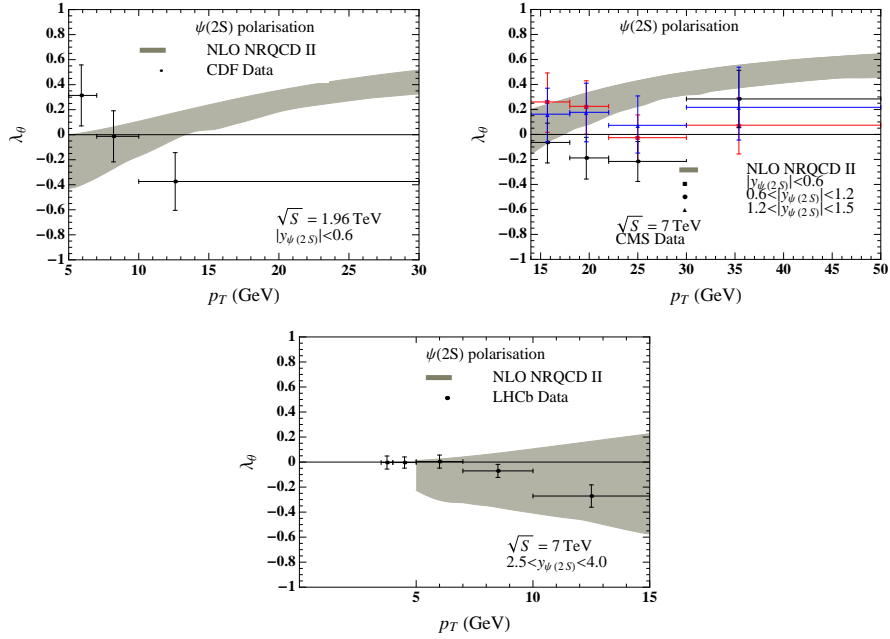
Figure 4: Comparison of NLO NRQCD (with the set II of CO LDMEs) and CDF [34], CMS [35] and LHCb [36] data for prompt $\psi(2S)$ polarisation λ_θ in helicity frame.

Later, we also consider the impact of feeddown contribution from χ_{cJ} decay on our direct J/ψ polarisation [12, 16]. From eq. (C4) in ref. [12], the feeddown contribution from χ_{c1} for J/ψ polarisation is in the interval $[-\frac{1}{3}, 1]$, while the feeddown contribution from χ_{c2} is in the interval $[-\frac{3}{5}, 1]$, regardless of its production mechanism.[3] We showed that the smearing from feeddown contribution will not change our result too much based on our direct J/ψ polarisation. Now, we are intending to give a rigorous prediction for prompt J/ψ yields and polarisation after including the feeddown contribution from χ_{cJ} and $\psi(2S)$ decay. As we discussed in section 2.2, the LDMEs of $M_{0,r_0}^{J/\psi}$ and $M_{1,r_1}^{J/\psi}$ are insensitive to the $p_{T\text{cut}}$ when $p_{T\text{cut}} > 7\text{GeV}$. We will use the values of $M_{0,r_0}^{J/\psi}$ and $M_{1,r_1}^{J/\psi}$ obtained from $p_T > 7\text{GeV}$ data only in this section.

4.1 yields

In this subsection, we present the p_T spectrum for prompt J/ψ yields. We show our NLO NRQCD predictions for prompt J/ψ yields in figure 5. The experimental data are taken from CDF [25], ATLAS [37], CMS [31] and LHCb [38]. Good agreement is found up to 70 GeV and in various rapidity bins.

In order to understand the fraction of feeddown contribution from χ_{cJ} to prompt J/ψ, we also show the theoretical prediction for $\frac{\sigma(\chi_c \to J/\psi\gamma)}{\sigma(J/\psi)}$ in figure 6 in the LHCb fiducial region. The plot implies that the p_T spectrum of prompt χ_c is harder than that of J/ψ, which can be understood as χ_c has a stronger p_T^{-4} behaviour. In figure 7, we also show the ratio R of prompt $\psi(2S)$ yields and prompt J/ψ yields as defined in refs. [32, 31],

$$R \equiv \frac{\sigma(\psi(2S) \to \mu^+\mu^-)}{\sigma(J/\psi \to \mu^+\mu^-)}, \tag{4.1}$$

which indicates the p_T dependence of feeddown contribution from $\psi(2S)$ in prompt J/ψ yields. With the default set of CO LDMEs for $\psi(2S)$, it increases as p_T becomes larger because of $M_{1,r_1}^{\psi(2S)}/M_{0,r_0}^{\psi(2S)} > M_{1,r_1}^{J/\psi}/M_{0,r_0}^{J/\psi}$. On the contrast, after using the new set II of CO LMDEs for $\psi(2S)$, the ratio R is flat in p_T, which is easily understood because of a smaller $M_{1,r_1}^{\psi(2S)}/M_{0,r_0}^{\psi(2S)}$. Finally, we divide the prompt J/ψ yields into direct J/ψ yields and the feeddown J/ψ from χ_c and $\psi(2S)$ decay in the second plot of figure 6. It shows that the p_T spectrum of feeddown J/ψ is harder than that of direct one.

Before going ahead into the discussion of the polarization case, we want to clarify that only the ratio R is sensitive to different sets of CO LMDEs for $\psi(2S)$ in this subsection, while other differential distributions are not. It is just because the feeddown contribution from $\psi(2S)$ in prompt J/ψ production is indeed small. This fact has also been checked numerically. It is also applicable to the polarization observable λ_θ for prompt J/ψ in the next subsection. Hence, we will refrain ourselves from

---

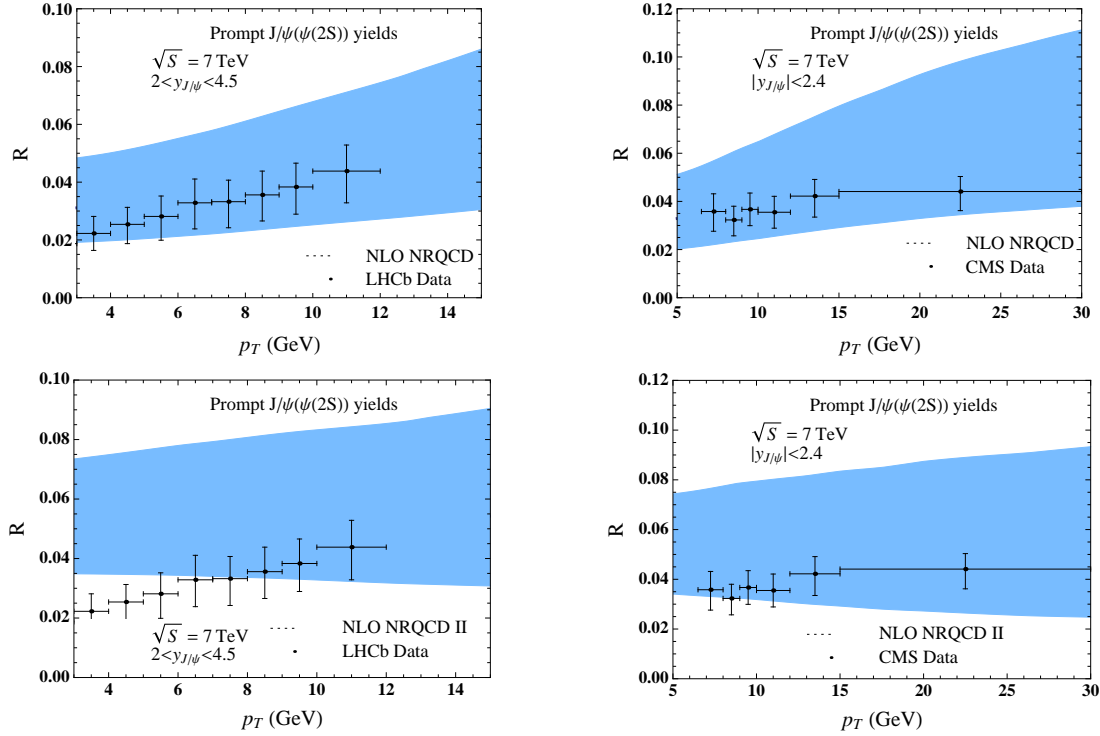[3]The J/ψ polarisation λ_θ from scalar particle χ_{c0} is always zero.
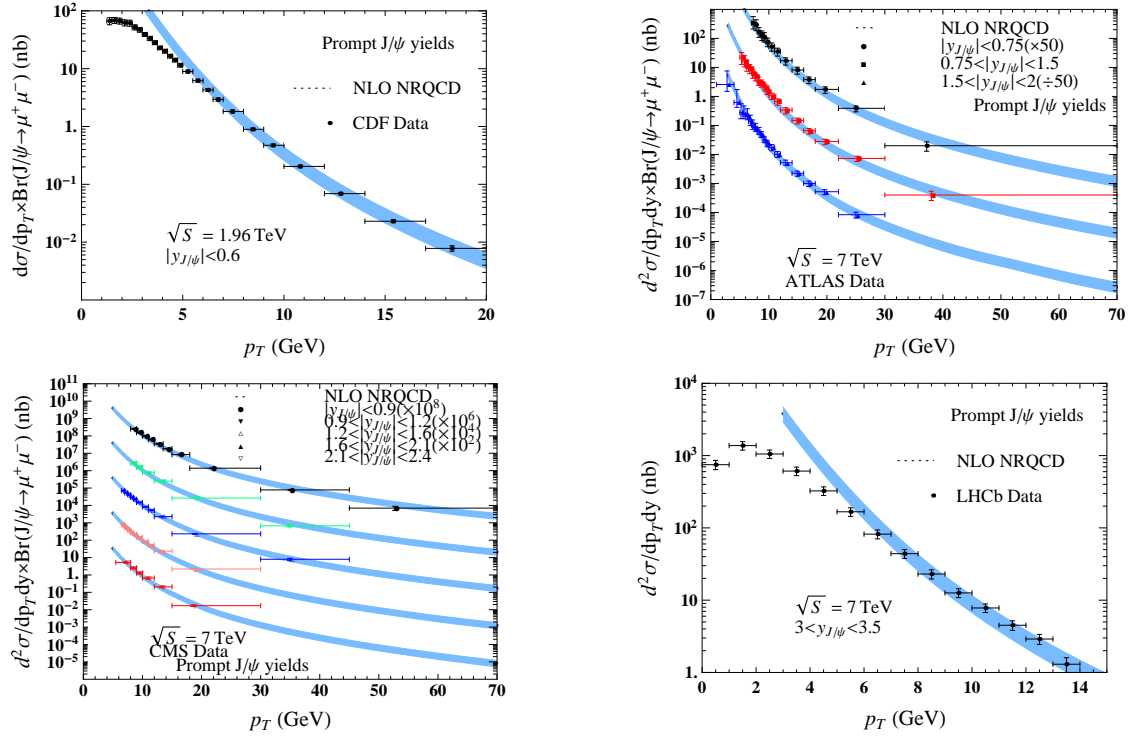
Figure 5: Comparison of NLO NRQCD and CDF [25],ATLAS [37],CMS [31] and LHCb [38] data for prompt J/ψ yields.
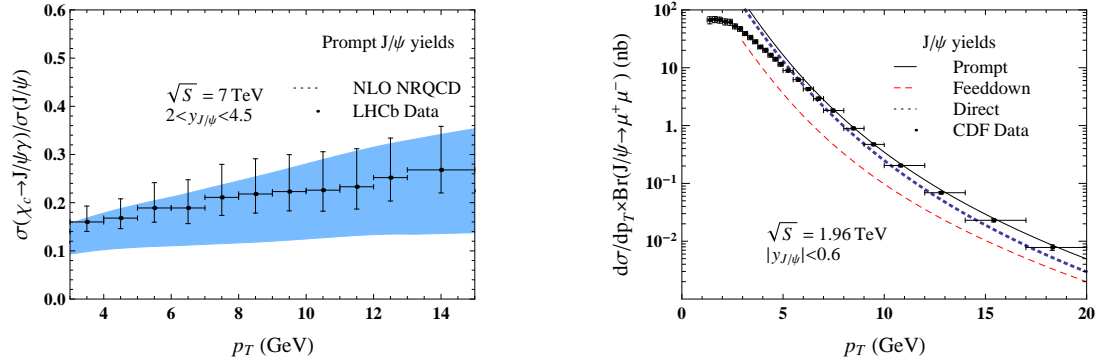
Figure 6: Comparison of NLO NRQCD and LHCb [39] and CDF [25] data for J/ψ yields.

presenting the similar plots by using the set II of CO LDMEs for $\psi(2S)$ except the ratio R.

Figure 7: Comparison of NLO NRQCD and LHCb [32] and CMS [31] data for R. We use the default set of CO LDMEs for $\psi(2S)$ in the upper two panels, while the lower two panels are obtained by using the set II of CO LDMEs for $\psi(2S)$.

4.2 polarizations

The polarisation for prompt J/ψ should be expected to be almost unpolarized because a smaller $M_{1,r_1}^{J/\psi}$ indicates a smaller transverse polarized component in prompt J/ψ. We compare our NLO NRQCD results with CDF [34], CMS [35], LHCb [40] and ALICE [41] data in figure 8. λ_θ in different rapidity bins are close to 0, which is consistent with our previous claim even after including feeddown contribution [6, 12]. Our results are in good agreement with the measurements of CMS [35],[4] LHCb [40] and ALICE [41] collaborations, while it is not so good with CDF data [34]. However, it is worthwhile to note that the CDF data is also inconsistent with the CMS data in the same rapidity interval.

Our positive LDMEs assumption is consistent with experiment that the LHCb data is a little bit lower than the CMS data. As we have pointed out in section 2, positivity of LDMEs implies that the λ_θ will be smaller in the forward rapidity bin than in the central rapidity bin, based on the understanding that $M_{1,r_1}^{J/\psi}$ is smaller

---

[4]Although there seems to be some difference between our theoretical results and the current CMS polarization data, we would like to mention that there are still some statistical fluctuations in the CMS data themselves, such as shown in the last bins in $|y| < 0.6$ and $0.6 < |y| < 1.2$ in figure 8.
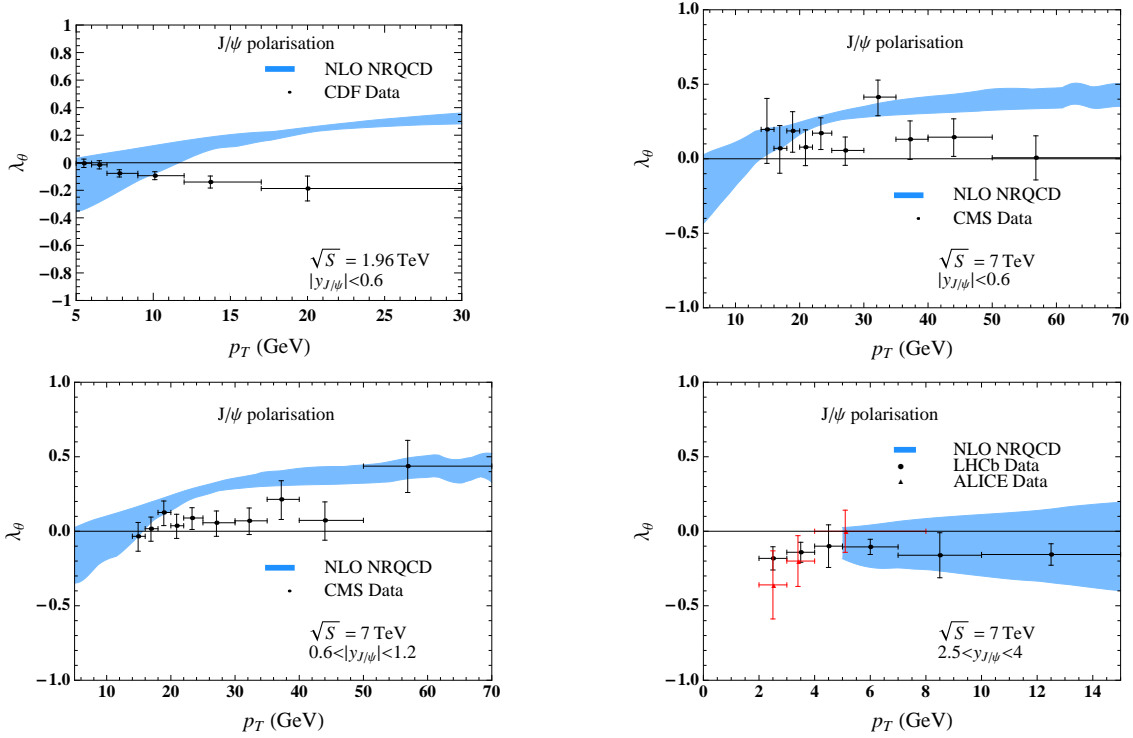
Figure 8: Comparison of NLO NRQCD and CDF [34],CMS [35], LHCb [40] and AL-ICE [41] data for prompt J/ψ polarisation λ_θ in helicity frame. The ALICE [41] data is for the inclusive J/ψ.

when rapidity y is larger. On the other hand, there are negative values of $\langle \mathcal{O}^{J/\psi}(^3P_0^{[8]})\rangle$ in the other two groups [5, 7]. They will give larger values of λ_θ in the forward rapidity bins, which will be in conflict with the LHCb data.

5. Summary

With large samples of heavy quarkonium accumulated at the LHC, quarkonium physics has reached the precision era even at large transverse momenta regime. In this article, we present a comprehensive analysis for prompt J/ψ and $\psi(2S)$ produced at the Tevatron and the LHC within NRQCD. For prompt J/ψ, we have taken feeddown contributions from $\chi_{cJ}(J = 0, 1, 2)$ and $\psi(2S)$ into account. Short-distance coefficients for all important CO Fock states are computed up to $\mathcal{O}(\alpha_S^4)$, i.e. at NLO in α_S. Color-singlet LDMEs of J/ψ, χ_{cJ} and $\psi(2S)$ are estimated by using potential model [22], while CO LDMEs are estimated by fitting experimental data. For $\chi_{cJ}(J = 0, 1, 2)$, there is only one independent CO LDME $\langle \mathcal{O}^{\chi_{c0}}(^3S_1^{[8]})\rangle$. Its value can be fixed by fitting the Tevatron data $\frac{\sigma(\chi_{c2}\to J/\psi\gamma)}{\sigma(\chi_{c1}\to J/\psi\gamma)}$ [23] as done in ref. [14]. For J/ψ or $\psi(2S)$, there are three independent CO LDMEs, i.e. $\langle \mathcal{O}^{J/\psi(\psi(2S))}(^1S_0^{[8]})\rangle$,

$\langle \mathcal{O}^{J/\psi(\psi(2S))}(^3S_1^{[8]})\rangle$ and $\langle \mathcal{O}^{J/\psi(\psi(2S))}(^3P_0^{[8]})\rangle$. From the decomposition of short-distance coefficients for $^3P_J^{[8]}$, we understand that it is difficult to extract the three independent CO LDMEs from the hadronic data even after including polarisation data. What we can determine unambiguously is two linear combinations of these three CO LDMEs. Their values were already extracted in refs. [8, 13] with $p_{T\text{cut}} = 7\text{GeV}$. However, we still need three CO LDMEs instead of two linear combinations to predict the yields and polarizations for prompt J/ψ and $\psi(2S)$ in various rapidity regions. We assume all CO LDMEs are of positive signs, which are in contrast to other groups' assumptions [5, 7]. The result obtained under our assumption is consistent with the observed relative magnitudes of polarization in the forward rapidity interval and in the central rapidity interval. Based on our assumption, we can provide more satisfactory predictions of both yields and polarizations λ_θ in the helicity frame for prompt J/ψ, which is almost unpolarized at hadron colliders. But we are unable to explain the polarization of prompt $\psi(2S)$ based on the old fit in ref. [8]. We thus checked the $\psi(2S)$ data and performed a new fit to the Tevatron data with $p_{T\text{cut}} = 11\text{GeV}$, which gives a better description for the polarization data of $\psi(2S)$.

However, on the theoretical side, it is still needed to understand why we have to use such a large p_T cutoff, which is much larger than the quarkonium mass. It might be possible that the NRQCD factorization formula may not be applicable if p_T is not large enough, which were also pointed out by the authors in refs. [10, 11]. Recently, it was found that the J/ψ production in small p_T regime may be described by a CGC+NRQCD formalism [42]. In a moderate p_T regime, say $p_T \sim 5 - 7\text{GeV}$, the CGC+NRQCD results match smoothly to our NLO NRQCD results [42], and thus the J/ψ production in the whole p_T regime may be described. It will be interesting to see whether the $\psi(2S)$ production in small and moderate p_T regime can be described in the same way. In recent years, several other efforts are made by people to understand the quarkonium production mechanism, including the relativistic corrections [43, 44], the small p_T regime resummation [45], and the large p_T regime factorization and resummation [46, 47, 48, 9, 49, 50, 51, 10, 52]. These works will provide more precise predictions for the quantitative understanding of quarkonium production. Moreover, other quarkonium associated production processes (e.g. double J/ψ production [53, 54, 55]) and/or other observables (e.g. fragmenting jet functions [56]) may also reveal the quarkonium production mechanism at the LHC in the future. On the experiment side, more precise measurements on the yields and especially the polarizations of heavy quarkonia are definitely needed to further clarify the present issues in quarkonium production.

Acknowledgments

References

[1] N. Brambilla, S. Eidelman, B. Heltsley, R. Vogt, G. Bodwin, et al., *Heavy quarkonium: progress, puzzles, and opportunities*, *Eur.Phys.J.* **C71** (2011) 1534, [arXiv:1010.5827].

[2] J. Lansberg, *J/ψ, ψ' and Υ production at hadron colliders: A Review*, *Int.J.Mod.Phys.* **A21** (2006) 3857–3916, [hep-ph/0602091].

[3] **CDF Collaboration** Collaboration, T. Affolder et al., *Measurement of J/ψ and $\psi(2S)$ polarization in $p\bar{p}$ collisions at $\sqrt{s} = 1.8$ TeV*, *Phys.Rev.Lett.* **85** (2000) 2886–2891, [hep-ex/0004027].

[4] G. T. Bodwin, E. Braaten, and G. P. Lepage, *Rigorous QCD analysis of inclusive annihilation and production of heavy quarkonium*, *Phys.Rev.* **D51** (1995) 1125–1171, [hep-ph/9407339].

[5] M. Butenschoen and B. A. Kniehl, *J/ψ polarization at Tevatron and LHC: Nonrelativistic-QCD factorization at the crossroads*, *Phys.Rev.Lett.* **108** (2012) 172002, [arXiv:1201.1872].

[6] K.-T. Chao, Y.-Q. Ma, H.-S. Shao, K. Wang, and Y.-J. Zhang, *J/ψ Polarization at Hadron Colliders in Nonrelativistic QCD*, *Phys.Rev.Lett.* **108** (2012) 242004, [arXiv:1201.2675].

[7] B. Gong, L.-P. Wan, J.-X. Wang, and H.-F. Zhang, *Polarization for Prompt J/ψ, $\psi(2s)$ production at the Tevatron and LHC*, *Phys.Rev.Lett.* **110** (2013) 042002, [arXiv:1205.6682].

[8] Y.-Q. Ma, K. Wang, and K.-T. Chao, *$J/\psi(\psi')$ production at the Tevatron and LHC at $\mathcal{O}(\alpha_s^4 v^4)$ in nonrelativistic QCD*, *Phys.Rev.Lett.* **106** (2011) 042002, [arXiv:1009.3655].

[9] Z. B. Kang, Y. Q. Ma, J. W. Qiu and G. Sterman, *Heavy Quarkonium Production at Collider Energies: Factorization and Evolution*, Phys. Rev. D **90**, 034006 (2014) arXiv:1401.0923.

[10] G. T. Bodwin, H. S. Chung, U. R. Kim and J. Lee, *Fragmentation contributions to J/psi production at the Tevatron and the LHC*, Phys. Rev. Lett. **113**, 022001 (2014) arXiv:1403.3612.

[11] P. Faccioli, V. Knnz, C. Lourenco, J. Seixas and H. K. Whri, *Quarkonium production in the LHC era: a polarized perspective*, Phys. Lett. B **736**, 98 (2014) arXiv:1403.3970.

[12] H. S. Shao and K. T. Chao, *Spin correlations in polarizations of P-wave charmonia χ_{cJ} and impact on J/ψ polarization*, Phys. Rev. D **90**, 014002 (2014) `arXiv:1209.4610`.

[13] Y.-Q. Ma, K. Wang, and K.-T. Chao, *A complete NLO calculation of the J/ψ and ψ' production at hadron colliders*, Phys.Rev. **D84** (2011) 114001, [`arXiv:1012.1030`].

[14] Y.-Q. Ma, K. Wang, and K.-T. Chao, *QCD radiative corrections to χ_{cJ} production at hadron colliders*, Phys.Rev. **D83** (2011) 111503, [`arXiv:1002.3987`].

[15] H.-S. Shao, *HELAC-Onia: An automatic matrix element generator for heavy quarkonium physics*, Comput.Phys.Commun. **184** (2013) 2562–2570, [`arXiv:1212.5293`].

[16] H. S. Shao, Y. Q. Ma, K. Wang and K. T. Chao, *Polarizations of χ_{c1} and χ_{c2} in prompt production at the LHC*, Phys. Rev. Lett. **112**, 182003 (2014) [`arXiv:1402.2913`].

[17] J. Pumplin, D. Stump, J. Huston, H. Lai, P. M. Nadolsky, et al., *New generation of parton distributions with uncertainties from global QCD analysis*, JHEP **0207** (2002) 012, [`hep-ph/0201195`].

[18] **Particle Data Group** Collaboration, K. Nakamura et al., *Review of particle physics*, J.Phys. **G37** (2010) 075021.

[19] M. Noman and S. D. Rindani, *Angular Distribution of Muons Pair Produced in pp Collisions*, Phys.Rev. **D19** (1979) 207.

[20] M. Beneke, M. Kramer, and M. Vanttinen, *Inelastic photoproduction of polarized J/ψ*, Phys.Rev. **D57** (1998) 4258–4274, [`hep-ph/9709376`].

[21] **CLEO Collaboration** Collaboration, M. Artuso et al., *Higher-order multipole amplitudes in charmonium radiative transitions*, Phys.Rev. **D80** (2009) 112003, [`arXiv:0910.0046`].

[22] E. J. Eichten and C. Quigg, *Quarkonium wave functions at the origin*, Phys.Rev. **D52** (1995) 1726–1728, [`hep-ph/9503356`].

[23] **CDF Collaboration** Collaboration, A. Abulencia et al., *Measurement of $\sigma_{\chi_{c2}}\mathcal{B}(\chi_{c2} \to J/\psi\gamma)/\sigma_{\chi_{c1}}\mathcal{B}(\chi_{c1} \to J/\psi\gamma)$ in $p\bar{p}$ collisions at $\sqrt{s} = 1.96$-TeV*, Phys.Rev.Lett. **98** (2007) 232001, [`hep-ex/0703028`].

[24] L. Jia, L. Yu and H. F. Zhang, *A global analysis of the experimental data on χ_c meson hadroproduction*, [`arXiv:1410.4032`].

[25] **CDF Collaboration** Collaboration, D. Acosta et al., *Measurement of the J/ψ meson and $b-$hadron production cross sections in $p\bar{p}$ collisions at $\sqrt{s} = 1960$ GeV*, Phys.Rev. **D71** (2005) 032001, [`hep-ex/0412071`].

[26] **CDF Collaboration** Collaboration, T. Aaltonen et al., *Production of $\psi(2S)$ Mesons in p anti-p Collisions at 1.96-TeV*, Phys.Rev. **D80** (2009) 031103, [arXiv:0905.1982].

[27] M. Butenschoen and B. A. Kniehl, *Reconciling J/ψ production at HERA, RHIC, Tevatron, and LHC with NRQCD factorization at next-to-leading order*, Phys.Rev.Lett. **106** (2011) 022003, [arXiv:1009.5662].

[28] M. Butenschoen and B. A. Kniehl, *World data of J/ψ production consolidate NRQCD factorization at NLO*, Phys.Rev. **D84** (2011) 051501, [arXiv:1105.0820].

[29] M. Butenschoen and B. A. Kniehl, *Next-to-leading-order tests of NRQCD factorization with J/ψ yield and polarization*, Mod.Phys.Lett. **A28** (2013) 1350027, [arXiv:1212.2037].

[30] R. Li and J. X. Wang, *Next-to-Leading-Order study on the associate production of $J/\psi + \gamma$ at the LHC*, Phys. Rev. D **89**, 114018 (2014) [arXiv:1401.6918].

[31] **CMS Collaboration** Collaboration, S. Chatrchyan et al., *J/ψ and ψ_{2S} production in pp collisions at $\sqrt{s} = 7$ TeV*, JHEP **1202** (2012) 011, [arXiv:1111.1557].

[32] **LHCb Collaboration** Collaboration, R. Aaij et al., *Measurement of $\psi(2S)$ meson production in pp collisions at sqrt(s)=7 TeV*, Eur.Phys.J. **C72** (2012) 2100, [arXiv:1204.1258].

[33] **ATLAS Collaboration** Collaboration, G. Aad et al., *Measurement of the production cross-section of $\psi(2S) \to J/\psi(\to \mu^+\mu^-)\pi^+\pi^-$ in pp collisions at $\sqrt{s} = 7$ TeV at ATLAS*, JHEP **1409** (2014) 079, [arXiv:1407.5532].

[34] **CDF Collaboration** Collaboration, A. Abulencia et al., *Polarization of J/ψ and ψ_{2S} mesons produced in $p\bar{p}$ collisions at $\sqrt{s} = 1.96$-TeV*, Phys.Rev.Lett. **99** (2007) 132001, [arXiv:0704.0638].

[35] **CMS Collaboration** Collaboration, S. Chatrchyan et al., *Measurement of the prompt J/ψ and $\psi(2S)$ polarizations in pp collisions at $\sqrt{s} = 7$ TeV*, Phys.Lett. **B727** (2013) 381–402, [arXiv:1307.6070].

[36] R. Aaij *et al.* [LHCb Collaboration], *Measurement of $\psi(2S)$ polarisation in pp collisions at $\sqrt{s} = 7$ TeV*, Eur. Phys. J. C **74**, 2872 (2014) [arXiv:1403.1339.

[37] **ATLAS Collaboration** Collaboration, G. Aad et al., *Measurement of the differential cross-sections of inclusive, prompt and non-prompt J/ψ production in proton-proton collisions at $\sqrt{s} = 7$ TeV*, Nucl.Phys. **B850** (2011) 387–444, [arXiv:1104.3038].

[38] **LHCb Collaboration** Collaboration, R. Aaij et al., *Measurement of J/ψ production in pp collisions at $\sqrt{s} = 7$ TeV*, Eur.Phys.J. **C71** (2011) 1645, [arXiv:1103.0423].

[39] **LHCb Collaboration** Collaboration, R. Aaij et al., *Measurement of the ratio of prompt χ_c to J/ψ production in pp collisions at $\sqrt{s} = 7$ TeV*, Phys.Lett. **B718** (2012) 431–440, [arXiv:1204.1462].

[40] **LHCb Collaboration** Collaboration, R. Aaij et al., *Measurement of J/ψ polarization in pp collisions at $\sqrt{s} = 7$ TeV*, Eur.Phys.J. **C73** (2013) 2631, [arXiv:1307.6379].

[41] **ALICE Collaboration** Collaboration, B. Abelev et al., *J/ψ polarization in pp collisions at $\sqrt{s} = 7$ TeV*, Phys.Rev.Lett. **108** (2012) 082001, [arXiv:1111.1630].

[42] Y. Q. Ma and R. Venugopalan, *Comprehensive Description of $J/$ Production in Proton-Proton Collisions at Collider Energies*, Phys. Rev. Lett. **113**, no. 19, 192301 (2014) arXiv:1408.4075.

[43] Y. Fan, Y.-Q. Ma, and K.-T. Chao, *Relativistic Correction to J/ψ Production at Hadron Colliders*, Phys.Rev. **D79** (2009) 114009, [arXiv:0904.4025].

[44] G.-Z. Xu, Y.-J. Li, K.-Y. Liu, and Y.-J. Zhang, *Relativistic Correction to Color Octet J/ψ Production at Hadron Colliders*, Phys.Rev. **D86** (2012) 094017, [arXiv:1203.0207].

[45] P. Sun, C.-P. Yuan, and F. Yuan, *Heavy Quarkonium Production at Low Pt in NRQCD with Soft Gluon Resummation*, Phys.Rev. **D88** (2013) 054008, [arXiv:1210.3432].

[46] Z. B. Kang, J. W. Qiu and G. Sterman, *Heavy quarkonium production and polarization*, Phys. Rev. Lett. **108** (2012) 102002 [arXiv:1109.1520].

[47] S. Fleming, A. K. Leibovich, T. Mehen, and I. Z. Rothstein, *The Systematics of Quarkonium Production at the LHC and Double Parton Fragmentation*, Phys.Rev. **D86** (2012) 094012, [arXiv:1207.2578].

[48] S. Fleming, A. K. Leibovich, T. Mehen and I. Z. Rothstein, *Anomalous dimensions of the double parton fragmentation functions*, Phys. Rev. **D 87**, 074022 (2013) [arXiv:1301.3822].

[49] Z. B. Kang, Y. Q. Ma, J. W. Qiu and G. Sterman, *Heavy Quarkonium Production at Collider Energies: Partonic Cross Section and Polarization*, arXiv:1411.2456.

[50] Y. Q. Ma, J. W. Qiu and H. Zhang, *Heavy quarkonium fragmentation functions from a heavy quark pair. I. S wave*, Phys. Rev. D **89**, 094029 (2014) arXiv:1311.7078.

[51] Y. Q. Ma, J. W. Qiu and H. Zhang, *Heavy quarkonium fragmentation functions from a heavy quark pair. II. P wave*, Phys. Rev. D **89**, 094030 (2014) arXiv:1401.0524.

[52] Y. Q. Ma, J. W. Qiu, G. Sterman and H. Zhang, *Factorized power expansion for high-p_T heavy quarkonium production*, Phys. Rev. Lett. **113**, 142002 (2014) arXiv:1407.0383.

[53] J. P. Lansberg and H. S. Shao, *Production of $J/\psi + \eta_c$ versus $J/\psi + J/\psi$ at the LHC: Importance of Real α_s^5 Corrections, Phys. Rev. Lett.* **111** (2013) 122001 `arXiv:1308.0474` .

[54] L. P. Sun, H. Han and K. T. Chao, *Impact of J/ψ pair production at the LHC and predictions in nonrelativistic QCD*, `arXiv:1404.4042`.

[55] J. P. Lansberg and H. S. Shao, *J/psi-Pair Production at Large Momenta: Indications for Double-Parton Scatterings and Large α_s^5 Contributions*, `arXiv:1410.8822`.

[56] M. Baumgart, A. K. Leibovich, T. Mehen and I. Z. Rothstein, JHEP **1411**, 003 (2014) [arXiv:1406.2295 [hep-ph]].